

# Metal sources of the Navan carbonate-hosted base metal deposit, Ireland: Nd and Sr isotope evidence for deep hydrothermal convection

R. D. Walshaw · J. F. Menuge · S. Tyrrell

Received: 26 April 2006 / Accepted: 11 September 2006 / Published online: 20 October 2006  
© Springer-Verlag 2006

**Abstract** Nd and Sr isotope analyses are presented for gangue mineral samples from the giant carbonate-hosted Navan Zn–Pb deposit, Ireland, and for rocks from which Navan metals may have been derived. Analysis of gangue minerals spanning the Navan paragenetic sequence reveals systematic evolution in the composition of the mineralising fluid. Early fluid represented by replacive dolomite exhibits the lowest initial  $^{87}\text{Sr}/^{86}\text{Sr}$  ratio (0.7083–0.7086), closest to that of the host limestone and to Lower Carboniferous seawater, and the highest  $^{143}\text{Nd}/^{144}\text{Nd}$  ratio (0.51161–0.51176). Later generations of dolomite, barite and calcite, which encompass sulphide precipitation, have higher initial  $^{87}\text{Sr}/^{86}\text{Sr}$  ratios (maximum 0.7105) and lower initial  $^{143}\text{Nd}/^{144}\text{Nd}$  ratios (minimum 0.51157). All samples have initial Nd isotope ratios that are too low to have been acquired only from the host limestone. Drill core samples of presumed Ordovician volcanic and sedimentary rocks from beneath the Navan orebody have  $^{143}\text{Nd}/^{144}\text{Nd}$  and  $^{87}\text{Sr}/^{86}\text{Sr}$  ratios at the time of mineralisation of 0.51184–0.51217 and 0.7086–0.7138, respectively. The data are interpreted to indicate mixing of sulphide-rich, limestone-buffered brine, with a metal-bearing hydrothermal fluid, which had passed through sub-Carboniferous rocks, consistent with published fluid inclusion and S isotope data. The  $^{143}\text{Nd}/^{144}\text{Nd}$  ratio of this basement-derived fluid is too

low to have been imparted by flow through the Devonian Old Red Sandstone, as required in models of regional fluid flow in response to Hercynian uplift. Irrespective of whether such regional fluid flow occurred, the hydrothermal Nd must have been derived from sub-Devonian rocks. These conclusions broadly support the hydrothermal convection cell model in which brines, ultimately of surface origin, penetrated to a depth of several kilometres, leaching metals from the rocks through which they passed. The data also support increasing depth of penetration of convection cells with time. Metals were subsequently precipitated in carbonate rocks at sites of mixing with cooler, sulphide-rich fluids. However, comparison of the Navan hydrothermal gangue Nd–Sr isotope data with data from Lower Palaeozoic rocks strongly suggests that the latter cannot alone account for the “basement” signature. As the Navan deposit lies immediately north of the Iapetus Suture, this suggests that the Laurentian margin includes Precambrian basement.

**Keywords** Zn–Pb mineralisation · Irish-type · Nd–Sr isotopes · Navan · Ireland

## Introduction

Irish-type ore deposits (Hitzman 1995a; Hitzman and Large 1986) represent a distinct style of hydrothermal mineralisation characterised by base metal sulphide precipitation relatively soon after deposition of the host carbonate sediments. They share many features in common with both the sedimentary exhalative and Mississippi Valley-type classes of deposit. They may be broadly subdivided into “stratabound” and “cross-cutting”, types where the former are hosted within Courceyan limestones, and the latter hosted partially within supra-Waulsortian facies of Chadian

Editorial handling: B. Lehmann

R. D. Walshaw  
LEMAS, Institute of Materials Research, University of Leeds,  
Leeds LS2 9JT, UK

J. F. Menuge (✉) · S. Tyrrell  
UCD School of Geological Sciences,  
University College Dublin, Belfield,  
Dublin 4, Ireland  
e-mail: j.f.menuge@ucd.ie

to Arundian age, although both subdivisions display strata-bound and crosscutting elements in their mineralisation. Mineralisation is spatially and temporally associated with extensional faulting, though the exact relationship between faulting and mineralisation remains contentious and may vary between deposits (e.g. Blakeman et al. 2002; Bonson et al. 2005; Peace and Wallace 2000).

Three types of genetic model have been proposed for the formation of the Irish-type deposits. These are the convection cell model (Russell 1978, 1986), the topography-driven fluid flow model (Garven and Freeze 1984a,b; Hitzman 1995a,b; Hitzman and Large 1986) and the stratal aquifer model (Lydon 1986). An understanding of the origin of the mineralising fluids, including their waters, metallic and non-metallic solutes, is essential to test any metallogenetic model. Fluid inclusion data for the Irish orefield define a negative correlation between temperature and salinity (Banks and Russell 1992; Everett et al. 1999; Eyre et al. 1996; Samson and Russell 1987) and have been interpreted by most workers as representing the mixing of two geochemically discrete fluids. The two proposed end members to this array are a high temperature (170–230°C), moderate salinity (8–12 wt% NaCl equiv.) fluid and a lower temperature (70–120°C), high salinity (17–28 wt% NaCl equiv.) fluid. Ore deposition in the Irish-type deposits appears to have been brought about predominantly by mixing of these two fluids.

The cool, high salinity fluid has been interpreted as a hypersaline brine immediately originating within the Lower Carboniferous carbonates (Samson and Russell 1987). It is often found as primary inclusions in paragenetically late minerals and as secondary inclusions in earlier minerals although both fluids are found throughout the mineral paragenesis on a regional scale. Low  $\delta D$  values in barite fluid inclusion leachates have been interpreted as either a meteoric fluid reacted with evaporites or a bacteriogenically altered seawater (Banks et al. 2002; Samson and Russell 1987). Evaporitic rocks, including halite pseudomorphs, have recently been reported in a mid-to late Chadian carbonate succession in County Carlow (Nagy et al. 2005). The combined C and O isotope study of Boast et al. (1981) identified Lower Carboniferous carbonate as one of the end members in an array displayed by ore-stage carbonate minerals. This end member could have been supplied by either the host rock or contemporaneous marine bicarbonate. A move towards  $\delta^{18}\text{O}$ - and  $\delta^{13}\text{C}$ -depleted values late in the paragenesis (post-ore carbonate) is interpreted as both mixing with bacterially oxidised carbon and the increasing influence of a deep-seated end member. Gleeson et al. (1999), working on samples from Tynagh, Silvermines and Lower Palaeozoic-hosted veins, have shown the halogen characteristics of fluid inclusion leachates to resemble evaporated seawater. Deviation of

some samples away from the seawater evaporation trajectory suggests various mixtures of seawater, bittern waters and meteoric water.

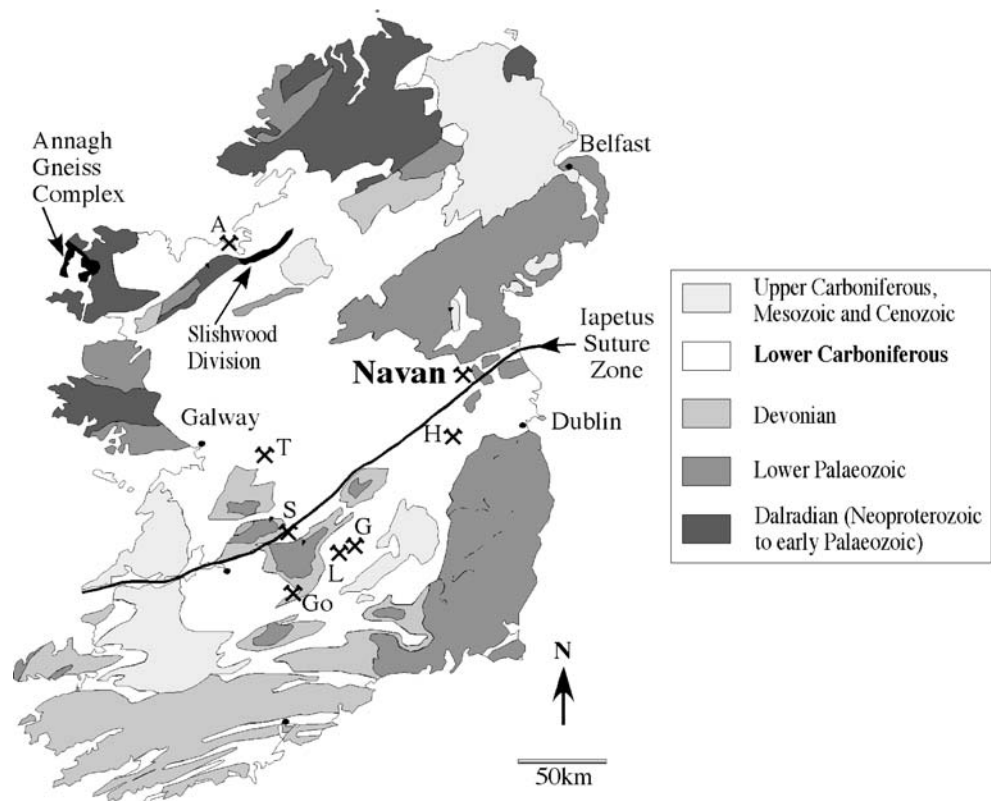
The origin of the hotter, less saline fluid is less well-understood. It has been suggested in the past to be a magmatic fluid (Samson and Russell 1987), a metamorphic formation water (Phillips 1983; Russell 1973) and a deeply circulated seawater (Russell 1978; Samson and Russell 1987). Due to the lack of any spatial association between any of the major base metal deposits and contemporaneous igneous activity, a magmatic source is very unlikely. Samson and Russell (1987) suggested that fluid inclusion homogenisation temperatures were incompatible with a magmatic model as was the major fluid inclusion cationic chemistry obtained via crush-leach analysis. These analyses showed that the fluid was similar to a fluid experimentally reacted with Irish Lower Palaeozoic greywacke by Bischoff et al. (1981); Ca/Na and K/Na ratios suggest that reaction with Lower Carboniferous carbonate or Old Red Sandstone feldspar was not significant. The fluid was also found by Samson and Russell (1987) to be in H and O isotopic equilibrium with Lower Palaeozoic basement lithologies. The question of whether this was a primary metamorphic formation water or a deeply circulated Lower Carboniferous seawater could not be resolved isotopically due to the possible loss of the original isotope composition of this fluid by interaction with the basement. However, they were able to rule out metamorphic formation waters on structural and volumetric grounds.

This paper presents Nd and Sr isotope analyses of the carbonate and barite gangue, which accompany hydrothermal Zn–Pb–Fe sulphide mineralisation in the Navan ore deposit and of whole-rock samples of the Lower Palaeozoic rocks forming the basement to the orebody. Supported by new and published Nd and Sr isotope data from regional pre-Carboniferous basement rocks, these data are used to constrain the origin of the base metals and, hence, the pathways followed by the hotter, metal-rich hydrothermal fluid.

### Previous studies of the Navan deposit

The Navan Zn–Pb deposit of County Meath, hosted in Lower Carboniferous carbonate sedimentary rocks (Fig. 1), is the largest carbonate-hosted base metal deposit in Ireland and is currently the largest Zn producer in Europe (Ashton et al. 2003). Mined ore, proven reserves and resources amount to about 95 Mt, grading 8.3% Zn and 2.1% Pb. Almost continuous mining since 1977, coupled with extensive exploration drill core, have allowed the stratigraphy, structure and mineralisation of the orebody to be described in considerable detail (Ashton et al. 2003).

**Fig. 1** Simplified geological map of Ireland, showing active and closed mines of base metal deposits hosted in Lower Carboniferous carbonate sedimentary rocks



In the Navan area, Lower Carboniferous sedimentary rocks lie unconformably on deformed Lower Palaeozoic rocks, both lying within a complex, faulted, SW-plunging antiform. The Lower Palaeozoic rocks form part of the Longford-Down Inlier. A NE-trending Ordovician succession includes sedimentary and basic to intermediate volcanic rocks and is enclosed to the NW and SE by Silurian greywackes, sandstones, siltstones and mudrocks (Vaughan 1991). Faunal, structural, isotopic and geophysical evidence suggests that the Lower Palaeozoic rocks lie just above the northward-dipping Iapetus Suture (Phillips 2001). A Precambrian gneissic basement at 3–4 km depth has been proposed on geophysical evidence (Williams and Brown 1986), but there are no exposures of Precambrian rocks.

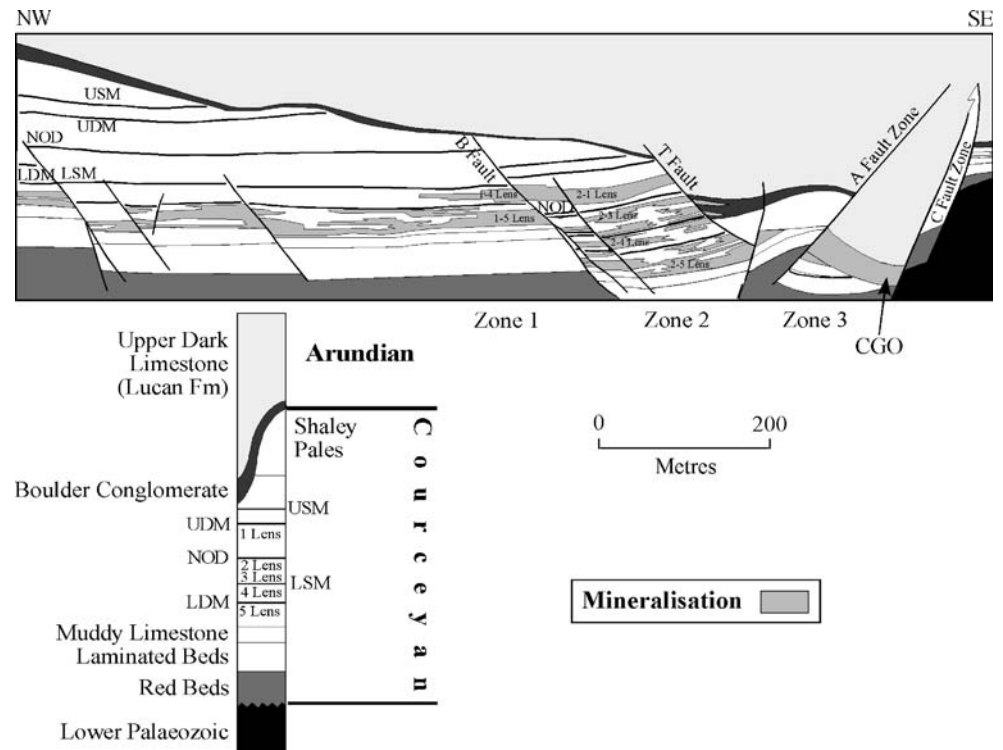
The Lower Carboniferous succession (Philcox 1984; Strogen et al. 1996) has been ascribed to a northerly marine transgression. The Courceyan Navan Group comprises thin red beds, succeeded in turn by a variety of thin carbonate and argillaceous beds known as the Pale Beds and the Shaley Pales. The orebody (Fig. 2) is hosted primarily in the Pale Beds, which comprise pale to medium grey micrites, oolitic and bioclastic calcarenites, dolomite, calcareous sandstones and minor shale-silt layers. The main orebody consists of a series of stratabound lenses divided into several zones by major NE to ENE-trending faults (Ashton et al. 2003). The ore is generally thickest adjacent to faults and dolomitised/argillaceous horizons, which appear to have acted as conduits and barriers,

respectively. Ore appears to have formed primarily by replacement of host limestones, with minor open space and late fracture-filling mineralisation. The Pale Beds are overlain successively by the Courceyan Shaley Pales, which contain minor economic mineralisation, and the Courceyan to Chadian Argillaceous Bioclastic Limestone (ABL) and Waulsortian Limestones. This succession has been truncated by a Chadian erosion surface on which was deposited the Boulder Conglomerate, a Chadian debris flow. Subordinate economic mineralisation occurs in the Boulder Conglomerate and is known as Conglomerate Group Ore (CGO).

The economic mineralogy is simple, consisting overwhelmingly of sphalerite and galena as ore with a Zn/Pb ratio of 5, occasionally with minor Ag sulphosalts. Pyrite and marcasite accompany the economic minerals, abundantly in the CGO and in subordinate quantities elsewhere. Gangue minerals include barite, calcite and dolomite.

The timing of mineralisation continues to be the subject of debate (Wilkinson 2003). Based on the relationship between mineralisation and faulting, which was active in Courceyan to Chadian times, most workers have argued that mineralisation began no later than during the Chadian (e.g. Blakeman et al. 2002; Coller et al. 2005). Mineralised clasts of Pale Beds in the CGO have been cited in support of this conclusion (Ashton et al. 2003). Other workers have concluded from a diagenetic study that all ore is post-Arundian in age (Peace and Wallace 2000) and it has been

**Fig. 2** Cross section of the Navan ore deposit, after Ashton et al. (1986)



proposed on palaeomagnetic grounds that the ores are late Arundian to early Asbian (Symons et al. 2002). However, a Lower Carboniferous age for the mineralisation is not in doubt, and the age uncertainty is not significant in the context of the present isotope study.

Published fluid inclusion data indicate fluids with homogenisation temperatures ( $T_h$ ) ranging from 75 to 220°C, broadly anti-correlated with salinity of 6–18 wt% NaCl equiv. (Everett et al. 1999). Sulphur in the Navan ore deposit can be interpreted as being of two origins (Anderson et al. 1998; Fallick et al. 2001). A seawater end member is manifested as both the isotopically light, bacteriogenically reduced sulphur found in sulphide minerals (having a  $\delta^{34}\text{S}$  of ca.  $-20\text{‰}$ ) and the heaviest (ca.  $+20\text{‰}$ ) sulphur found as sulphate, exclusively in late barite. A second source of sulphur with  $\delta^{34}\text{S}$  values clustering around  $+10$  is proposed to have originated in the basement and travelled in solution with dissolved metals. This sulphur is isotopically very similar to that in diagenetic pyrite found in a variety of Lower Palaeozoic rocks and is dominant early in the paragenesis (Anderson et al. 1998; Fallick et al. 2001; Blakeman et al. 2002). Compared with the bacteriogenic sulphur component, the basement-derived sulphur is volumetrically minor, and it seems that a continuous source of bacteriogenic sulphur was an essential requirement for the development of a large orebody at Navan (Anderson et al. 1998; Fallick et al. 2001). Pb isotope analysis of Navan galena is also consistent with derivation of the Pb and presumably the other ore metals,

from local Silurian and Ordovician sedimentary and volcanic rocks (O’Keeffe 1986).

### Sample collection and analytical methods

Rb–Sr and/or Sm–Nd isotopes were determined on mineral and whole-rock samples. The procedures employed for mineral separation, dissolution, chemical separation and thermal ionisation mass spectrometry varied according to sample type. Procedures for Rb–Sr analysis of sphalerite leachates were developed specifically for this project and are described in detail; brief accounts are given for the other procedures, which are variants on published techniques.

#### Sample collection and mineral separation

##### *Hydrothermal mineralisation*

Gangue mineral and sphalerite samples spanning the paragenetic sequence were collected from mineralisation hosted in the Pale Beds in the main Navan orebody. Sampling locations are shown on the cross-section of the deposit (Fig. 2). A paragenetic sequence for the Navan deposit has been assembled from Hitzman (1995a), Braithwaite and Rizzi (1997) and petrography carried out during this study. Using cathodoluminescence, Braithwaite and Rizzi (1997) identified three stages of dolomitisation at Navan, the latest of which overlaps with sulphide precipitation. Late-stage

honeyblende overgrows late dolomite and is in turn overgrown by calcite and barite; calcite and barite also commonly overgrow colloform sphalerite, in some cases with an intervening or contemporaneous episode of sulphide dissolution. The length of time over which sphalerite was being precipitated is unconstrained and was possibly quite prolonged. All calcites have a similar orange cathodoluminescence and are indistinguishable. For the purposes of expressing isotope compositions through time, this paragenesis is split into seven stages as follows:

- 0 Host rock
- 1 Replacive dolomite (stage 1 of Braithwaite and Rizzi 1997)
- 2 Dolomite (stage 2 of Braithwaite and Rizzi 1997)
- 3 Sulphides (generally typified by massive/replacive forms)
- 4 Saddle dolomite (+ bitumen; Stage 3 of Braithwaite and Rizzi 1997)
- 5 Sulphides (typically fine–coarse honeyblende)
- 6 Barite/calcite
- 7 Later calcite

Making clear distinctions between the paragenetic stages in different hand specimens is sometimes difficult, and it is quite likely that variable degrees of temporal overlap existed between the different stages. The paragenetic stage for each mineral sample is shown in Table 1.

It has been shown by a number of studies, reviewed by Walshaw and Menuge (1998), that sphalerite fluid inclusions in carbonate-hosted base metal deposits have very low Rb/Sr ratios. Consequently, sphalerite fluid inclusion contents retain the initial  $^{87}\text{Sr}/^{86}\text{Sr}$  ratios from which they crystallised and can be liberated by crushing and leaching. Sphalerites for crush-leach Rb–Sr isotope analysis were prepared either by roughly crushing selected hand specimens in a steel pestle and mortar or by cutting from thick sections using a scalpel and then crushing. These samples were then handpicked under a binocular microscope to exclude solid inclusions of exotic material from the sample. All other mineral samples were extracted by handpicking from crushed and sieved rock samples.

#### *Whole-rock samples*

Localities at which whole-rock samples were collected are given in Table 2, along with brief lithological descriptions and stratigraphic positions. Two samples of unmineralised Lower Carboniferous Waulsortian micritic limestones and a single sample of argillaceous limestone from the Argillaceous Bioclastic Limestone were collected. Ten samples collected from the Upper Devonian Old Red Sandstone of the Munster basin cover most of the stratigraphic range. Five samples of Silurian sedimentary rocks were collected

from the Irish midlands. Six drill core samples of presumed Ordovician volcanic and sedimentary rocks from beneath the main Navan orebody were sampled from drill core U9555 as examples of its local basement. The core was extracted from beneath Zone 2 (Ashton et al. 1986) of the orebody and the sample numbers are the depth in meters beneath the top of the hole at which the sample was collected; the samples analysed were taken from below Zone 1. The volcanic and volcanogenic rocks exhibit secondary alteration probably developed during seafloor metamorphism. However, none of the samples contain significant quantities of sulphide minerals or other hydrothermal minerals related to Navan mineralisation.

#### *Dissolution and ion chromatographic separation procedures*

In all cases, mixed  $^{87}\text{Rb}$ – $^{84}\text{Sr}$  and/or mixed  $^{147}\text{Sm}$ – $^{150}\text{Nd}$  spike solutions were added to samples before dissolution and separation. Two types of ion chromatographic material were used: Dowex Bio-Rad AG50W-X12 200–400 mesh ion exchange resin and the ion-specific resins SrSPEC<sup>TM</sup>, TruSPEC<sup>TM</sup> and LN resin<sup>TM</sup> supplied by Eichrom Technologies.

#### *Sphalerites*

Samples were leached with 10% acetic acid overnight at 80°C, including agitation in an ultrasonic bath to remove any adhering fine-grained carbonate, and then rinsed in distilled water. The clean sphalerite residue was then crushed to powder using a boron carbide mortar and pestle. The powder was slurried with distilled water and leached overnight, centrifuged and the leachate retained. The residue was leached again overnight with distilled water, centrifuged and the second leachate mixed with the first and spiked with a dilute mixed Rb–Sr spike solution.

The very small amounts of Sr in sphalerite leachates were separated via a single pass through very small SrSPEC columns (containing 55  $\mu\text{l}$  resin when wet). These columns were constructed by slurring SrSPEC in water, washing it in 3 M HNO<sub>3</sub> before loading it into polytetrafluoroethylene (PTFE) microcolumns with a pipette, taking care to avoid introduction of air bubbles to the resin bed. Columns were then cleaned with three reservoir volumes of 3 M HNO<sub>3</sub> followed by two reservoir volumes of distilled H<sub>2</sub>O. Sr elution was carried out using a total volume of 1.066 ml distilled 3 M HNO<sub>3</sub> to load and wash on the sample, followed by 200  $\mu\text{l}$  of distilled H<sub>2</sub>O to release the Sr from the resin.

A Rb fraction was also collected from the SrSPEC columns and then purified by passing twice dissolved in HCl through a larger column packed with 3 g of Dowex cation exchange resin. The Dowex resin in these columns

**Table 1** Rb–Sr and Sm–Nd isotope data for Navan gangue minerals and sphalerite fluid inclusion leachates

| Sample no. | Grid ref. location/mine coordinate        | Mineral   | Paragenetic stage | $^{87}\text{Sr}/^{86}\text{Sr}$ | Rb (ppm) | Sr (ppm) | $^{87}\text{Rb}/^{86}\text{Sr}$ | $^{87}\text{Sr}/^{86}\text{Sr}$ (350) | $^{143}\text{Nd}/^{144}\text{Nd}$ | Sm (ppm) | Nd (ppm) | $^{147}\text{Sm}/^{144}\text{Nd}$ | $^{143}\text{Nd}/^{144}\text{Nd}$ (350) | $\epsilon_{\text{Nd}}$ (350) |
|------------|---|-----------|-------------------|---------------------------------|----------|----------|---------------------------------|---------------------------------------|-----------------------------------|----------|----------|-----------------------------------|---|------------------------------|
| N1149.529A | DDH 1149, 529 m, U-lens                   | Ca        | 7                 | 0.71000 [2]                     | 0.0294   | 104.9    | 0.0008                          | 0.71000                               | 0.511843 [18]                     | 3.186    | 16.04    | 0.1200                            | 0.511568                                | -12.1                        |
| N1149.529B |   | Ca        | 6                 | 0.70929 [8]                     | 0.0048   | 382.4    | 0.0000                          | 0.70929                               | 0.511874 [16]                     | 1.256    | 5.621    | 0.1350                            | 0.511565                                | -12.2                        |
| N1099.455A | DDH 1099, 455 m (fault zone in Pale Beds) | Dol       | 2                 | 0.70945 [14]                    | 0.0851   | 26.27    | 0.0094                          | 0.70940                               | 0.511986 [14]                     | 1.384    | 6.531    | 0.1280                            | 0.511692                                | -9.7                         |
| N1099.455B |   | Dol       | 1                 | 0.70874 [4]                     | 1.486    | 60.11    | 0.0587                          | 0.70830                               | 0.511910 [18]                     | 0.4928   | 2.450    | 0.1214                            | 0.511614                                | -10.9                        |
| N1099.455C |   | Ca        | 6                 | 0.71031 [6]                     | 0.5170   | 152.2    | 0.0098                          | 0.71026                               |                                   |          |          |                                   |   |                              |
| W8/94-N4   | 1–5 lens                                  | Dol       | 1                 | 0.70864 [3]                     | 1.263    | 153.4    | 0.0238                          | 0.70852                               | 0.511923 [25]                     | 0.8075   | 3.995    | 0.1222                            | 0.511643                                | -10.6                        |
| N1141A     | DDH 1141, 386 m, P Fault zone             | Dol       | 4                 | 0.71014 [40]                    | 0.0303   | 32.24    | 0.0027                          | 0.71014                               | 0.511983 [32]                     | 1.164    | 4.445    | 0.1582                            | 0.511620                                | -11.1                        |
| N1141B     |   | Ca        | 6                 | 0.71052 [32]                    | 0.0127   | 97.50    | 0.0004                          | 0.71052                               | 0.512045 [16]                     | 1.917    | 7.418    | 0.1562                            | 0.511687                                | -9.8                         |
| W3/94-N1   | 1315 252                                  | Dol       | 1                 | 0.70859 [5]                     | 0.8440   | 338.7    | 0.0072                          | 0.70856                               | 0.512028 [18]                     | 0.6279   | 3.196    | 0.1187                            | 0.511756                                | -8.4                         |
| W8/94-N5   | 1159 2011                                 | Ca        | 6                 | 0.70823 [7]                     | 0.0558   | 627.8    | 0.0003                          | 0.70823                               | 0.511918 [12]                     | 1.368    | 8.065    | 0.1025                            | 0.511683                                | -9.9                         |
| F26        | F26 fault                                 | Ca        | 6                 | 0.70927 [3]                     | 0.0251   | 115.6    | 0.0006                          | 0.70927                               | 0.511962 [20]                     | 0.8853   | 3.740    | 0.1430                            | 0.511634                                | -10.8                        |
| C1         | 2–3 lens                                  | Ca        | 6                 | 0.70939 [6]                     | 34.78    | 522.2    | 0.1927                          | 0.70843                               |                                   |          |          |                                   |   |                              |
| C2         | 2–3 lens                                  | Ca        | 6                 | 0.70895 [3]                     | 0.0317   | 109.7    | 0.0008                          | 0.70895                               |                                   |          |          |                                   |   |                              |
| W8/94-N9   | 1230 261, 2–5 lens                        | Ba        | 6                 | 0.70878 [3]                     | 10.00    | 301.5    | 0.0010                          | 0.70877                               |                                   |          |          |                                   |   |                              |
| W8/94-N7   | 1315, 2–1 lens                            | Ba        | 6                 | 0.70843 [3]                     | 10.00    | 5237     | 0.0006                          | 0.70842                               |                                   |          |          |                                   |   |                              |
| W3/94-N2   | 1315 255                                  | Ba        | 6                 | 0.70843 [3]                     | 10.00    | 4822     | 0.0006                          | 0.70843                               |                                   |          |          |                                   |   |                              |
| W11/94-N1  | 1300 211, P4 2–1 lens                     | Sp leach. | 5                 | 0.70846 [13]                    | 0.0129   | 1.763    | 0.0212                          | 0.70836                               |                                   |          |          |                                   |   |                              |
| W11/94-N1  | (1)                                       | Sp leach. | 5                 | 0.70853 [25]                    | 0.0977   | 1.902    | 0.1487                          | 0.70779                               |                                   |          |          |                                   |   |                              |
| W11/94-N1  | (2)                                       | Sp leach. | 5                 | 0.70824 [20]                    | 0.0282   | 5.762    | 0.0142                          | 0.70817                               |                                   |          |          |                                   |   |                              |
| W11/94-N1  | (3)                                       | Sp leach. | 5                 | 0.70842 [34]                    | 0.0201   | 18.52    | 0.0031                          | 0.70840                               |                                   |          |          |                                   |   |                              |
| W8/94-N3   | 1315 255, 2–3 lens                        | Sp leach. | 5                 | 0.70842 [34]                    | 0.0201   | 18.52    | 0.0031                          | 0.70840                               |                                   |          |          |                                   |   |                              |

Figures in brackets denote internal precision ( $2\sigma$ ).  $^{87}\text{Sr}/^{86}\text{Sr}$ (350),  $^{143}\text{Nd}/^{144}\text{Nd}$ (350), and  $\epsilon_{\text{Nd}}$  (350) are initial values for  $T=350$  Ma.

**Table 2** Rb–Sr and Sm–Nd isotope data for host and basement whole-rock samples

| Sample number   | Lithology, formation                         | Locality/grid reference             | $^{87}\text{Sr}/^{86}\text{Sr}^*$ | Rb (ppm) | Sr (ppm) | $^{87}\text{Rb}/^{86}\text{Sr}$ | $^{87}\text{Sr}/^{86}\text{Sr}$ (350) | $^{143}\text{Nd}/^{144}\text{Nd}^*$ | Sm (ppm) | Nd (ppm) | $^{147}\text{Sm}/^{144}\text{Nd}$ | $^{143}\text{Nd}/^{144}\text{Nd}$ (350) | $\epsilon_{\text{Nd}}$ (350) |
|---|--|-------------------------------------|-----------------------------------|----------|----------|---------------------------------|---------------------------------------|-------------------------------------|----------|----------|-----------------------------------|---|------------------------------|
| Lower Carboniferous   |  |                                     |                                   |          |          |                                 |                                       |                                     |          |          |                                   |   |                              |
| W3347   | Argillite, Argillaceous bioclastic limestone | Drill hole 91–3347–1 Navan          | 0.72183 [5]                       | 259.2    | 283.2    | 2.652                           | 0.70862                               | 0.511742 [18]                       | 3.464    | 21.16    | 0.0989                            | 0.511515                                | –13.1                        |
| WTwm  | Micrite, Waulsortian                         | Woodtown, Co. Meath                 | 0.70789 [5]                       | 0.342    | 175.8    | 0.0056                          | 0.70786                               | 0.512059 [26]                       | 0.154    | 0.776    | 0.1200                            | 0.511784                                | –7.9                         |
| TM  | Micrite, Waulsortian                         | Tynagh, Co. Galway                  | 0.70861 [3]                       | 1.690    | 226.6    | 0.0216                          | 0.70851                               | 0.511997 [34]                       | 1.257    | 5.693    | 0.1335                            | 0.511691                                | –9.7                         |
| Devonian Old Red Sandstone, Munster Basin (all sandstones)        |  |                                     |                                   |          |          |                                 |                                       |                                     |          |          |                                   |   |                              |
| ST308   | Old Head Sandstones                          | Baltimore 11445 02727               | 0.77813 [4]                       | 26.77    | 5.641    | 13.83                           | 0.70923                               | 0.512108 [14]                       | 6.113    | 34.05    | 0.1085                            | 0.511859                                | –6.4                         |
| ST301   | Toe Head sandstones                          | Roaringwater Bay 10595 02612        |                                   |          |          |                                 |                                       | 0.512122 [18]                       | 1.643    | 6.183    | 0.1607                            | 0.511754                                | –8.5                         |
| ST303   | Toe Head Sandstones                          | Roaringwater Bay 11445 02727        |                                   |          |          |                                 |                                       | 0.512086 [10]                       | 12.46    | 66.66    | 0.1130                            | 0.511827                                | –7.0                         |
| ST310   | Toe Head sandstones                          | Toe Head 11430 02735                |                                   |          |          |                                 |                                       | 0.512196 [10]                       | 10.62    | 42.49    | 0.1511                            | 0.511850                                | –6.6                         |
| ST312   | Toe Head Sandstones                          | Galley Head 13466 03231             | 0.77287 [9]                       | 36.81    | 8.264    | 12.97                           | 0.70825                               | 0.512066 [12]                       | 7.202    | 38.44    | 0.1133                            | 0.511806                                | –7.4                         |
| ST313   | Toe Head Sandstones                          | Galley Head 13572 03282             |                                   |          |          |                                 |                                       | 0.512086 [20]                       | 8.624    | 49.14    | 0.1061                            | 0.511843                                | –6.7                         |
| ST306   | Sherkin Formation                            | Baltimore 10595 02595               |                                   |          |          |                                 |                                       | 0.512061 [18]                       | 2.731    | 12.62    | 0.1309                            | 0.511761                                | –8.3                         |
| ST307   | Castlehaven Formation                        | Baltimore 10525 03050               |                                   |          |          |                                 |                                       | 0.512000 [14]                       | 4.092    | 19.89    | 0.1244                            | 0.511715                                | –9.2                         |
| W6/98-CP1   | Dingle Beds                                  | Connor Pass 066 504                 | 0.75381 [7]                       | 132.1    | 48.68    | 7.886                           | 0.71452                               | 0.512062 [12]                       | 5.370    | 27.03    | 0.1201                            | 0.511787                                | –7.8                         |
| W6/98-CP2   | Dingle Beds                                  | Connor Pass 066 504                 | 0.73387 [5]                       | 105.3    | 90.22    | 3.387                           | 0.71700                               | 0.512069 [08]                       | 5.192    | 26.35    | 0.1191                            | 0.511796                                | –7.6                         |
| Silurian, Co. Tipperary   |  |                                     |                                   |          |          |                                 |                                       |                                     |          |          |                                   |   |                              |
| W4/98-BQ5   | Slate, Hollyford Fm                          | Birdhill 173 169                    | 0.74570 [7]                       | 127.5    | 62.64    | 5.911                           | 0.71625                               | 0.512040 [19]                       | 5.295    | 27.55    | 0.1162                            | 0.511774                                | –8.1                         |
| W3/98-SB2   | Greywacke, Hollyford Fm                      | Kinnity Forest 224 204              | 0.71379 [4]                       | 53.55    | 187.7    | 0.8259                          | 0.70967                               | 0.512111 [14]                       | 3.851    | 20.83    | 0.1120                            | 0.511855                                | –6.5                         |
| W4/98-AM1   | Mudstone, Broadford Fm                       | Arra Mountains 1720 1745            | 0.71984 [3]                       | 11.18    | 211.2    | 0.1534                          | 0.71908                               | 0.512063 [16]                       | 11.53    | 59.82    | 0.1165                            | 0.511796                                | –7.6                         |
| W4/98-AM2   | Greywacke, Slieve Bernagh Fm                 | Graves of the Leinstermen 1730 1770 | 0.71236 [2]                       | 42.18    | 286.6    | 0.4260                          | 0.71024                               | 0.512097 [18]                       | 5.322    | 27.73    | 0.1160                            | 0.511831                                | –7.0                         |
| W4/98-AM4   | Slate, Slieve Bernagh Fm                     | Graves of the Leinstermen 1735 1782 | 0.73506 [6]                       | 133.2    | 103.3    | 3.739                           | 0.71643                               | 0.512060 [17]                       | 5.371    | 27.44    | 0.1183                            | 0.511789                                | –7.8                         |
| Ordovician basement from core U9555, Tara Mines, Navan, Co. Meath |  |                                     |                                   |          |          |                                 |                                       |                                     |          |          |                                   |   |                              |
| 111.5   | Volcanogenic sediment                        | Tara Mines core U9555               | 0.73923 [50]                      | 250.0    | 129.0    | 5.626                           | 0.71120                               | 0.512269 [16]                       | 4.788    | 25.90    | 0.1242                            | 0.511984                                | –4.0                         |
| 140.0   | Red siltstone                                | Tara Mines core U9555               | 0.75646 [32]                      | 253.3    | 96.94    | 7.597                           | 0.71860                               | 0.512051 [10]                       | 7.103    | 37.05    | 0.1159                            | 0.511785                                | –7.9                         |
| 177.3   | Felsic vitric tuff                           | Tara Mines core U9555               | 0.71544 [40]                      | 70.09    | 148.4    | 1.368                           | 0.70863                               | 0.512388 [20]                       | 2.625    | 16.44    | 0.0966                            | 0.512167                                | –0.4                         |
| 188.0   | Green siltstone                              | Tara Mines core U9555               | 0.73261 [64]                      | 178.9    | 133.7    | 3.880                           | 0.71328                               | 0.512144 [18]                       | 9.003    | 41.17    | 0.1322                            | 0.511841                                | –6.8                         |
| 208.5   | Volcanic agglomerate                         | Tara Mines core U9555               | 0.71325 [30]                      | 119.6    | 307.8    | 1.125                           | 0.70764                               | 0.512445 [14]                       | 5.399    | 26.74    | 0.1221                            | 0.512166                                | –0.4                         |
| 229.9   | Coarse volcanic agglomerate                  | Tara Mines core U9555               | 0.70956 [36]                      | 106.4    | 689.2    | 0.447                           | 0.707340                              | 0.512466 [12]                       | 4.421    | 21.51    | 0.1243                            | 0.512181                                | –0.1                         |

Figures in brackets denote internal precision ( $2\sigma$ ).  $^{87}\text{Sr}/^{86}\text{Sr}(350)$ ,  $^{143}\text{Nd}/^{144}\text{Nd}(350)$ , and  $\epsilon_{\text{Nd}}$  (350) are initial values for  $T=350$  Ma

was carefully cleaned before use by two cycles of different concentrations of HCl, beginning with distilled H<sub>2</sub>O progressing through 1, 2, 3 and finally 6 M HCl. This process expands and contracts the resin, thus aiding the removal of blank Rb.

#### *Other minerals and whole rocks*

Powdered barite samples were dissolved using the method established by O’Keeffe (1987). Fifty-milligram samples were dissolved in 1.5 ml of hot concentrated H<sub>2</sub>SO<sub>4</sub>; 15 ml of 1 M Na<sub>2</sub>CO<sub>3</sub> was added and the solution was boiled for 1 h to convert SrSO<sub>4</sub> to SrCO<sub>3</sub>. Twenty millilitres of deionised water was then added to dissolve the highly soluble Na<sub>2</sub>SO<sub>4</sub>. The solution was decanted and another 20 ml deionised water was added. This too was decanted and the decanted solution was discarded. The SrCO<sub>3</sub> residue was then dissolved in 3 ml of 2.5 M HCl. Carbonate mineral and rock samples were dissolved in 1 M HCl rather than HF to minimise the risk of contamination via dissolution of silicate impurities. Silicate whole-rock powders were dissolved conventionally using concentrated HF, HNO<sub>3</sub> and HCl (Menuge 1988).

Two ion chromatography protocols were employed at different times. Under the earlier protocol, columns containing 5 g of Dowex AG50W-X12 resin and HCl and HNO<sub>3</sub> eluents were used to separate Rb, Sr, and rare earth elements (REE; Sm and Nd). The Rb and Sr fractions collected were passed again through the same columns with HCl to produce Rb and Sr pure enough for mass spectrometry. Separation of Sm and Nd from the REE fraction from the Dowex column was effected by a single pass through a second column filled with Voltalef 300 LD PL micro PTFE powder coated with di-(2-ethylhexyl) phosphate. Elution was carried out using dilute HCl of variable concentrations. This yielded Sm and Nd of sufficient purity for mass spectrometry.

The later protocol used small SrSPEC columns piggy-backed over small TruSPEC columns, based on the method of Pin et al. (1994). These are ion-specific “resins”, which extract Sr and REE, respectively, from HNO<sub>3</sub> solutions by complexation. One hundred milligrams of the resin was used in both columns. Rb passes through both columns and was purified as in the old protocol by two passes through a 5-g Dowex column after conversion to chloride. Sr and REE were eluted from the ion-specific resins by 0.05 M HNO<sub>3</sub>. In the case of the REE fraction, the TruSPEC columns were piggybacked above columns containing LN resin; the REE, through the addition of 0.05 M HNO<sub>3</sub>, were washed directly onto the LN columns. Sm and Nd were then separated from each other and from other REE on the LN columns by elution with HCl. In the case of silicate whole rocks, the Sr fraction required only a second pass

through the same SrSPEC column before it was sufficiently pure for mass spectrometry. In the case of carbonate rock and mineral samples, after two passes through SrSPEC columns, the Sr fractions were passed once through the 5-g Dowex columns to further purify the Sr before mass spectrometry. This was necessary due to the inability of SrSPEC to completely remove Ca from the Sr fraction in high Ca samples; Ca within the Sr fraction inhibits the ionisation of Sr within the mass spectrometer leading to unsatisfactory analysis.

#### Mass spectrometry

All samples were analysed on a partially automated VG Micromass 30 thermal ionisation mass spectrometer equipped with a single Faraday collector. The sample loading and running conditions for all samples except sphalerite leachates are as outlined in Menuge (1988). All <sup>87</sup>Sr/<sup>86</sup>Sr ratios were corrected to an SRM987 <sup>87</sup>Sr/<sup>86</sup>Sr value of 0.710300. External reproducibility of <sup>87</sup>Sr/<sup>86</sup>Sr ratios, based on replicate analyses of SRM 987, is estimated to be ±0.00010 or the internal precision quoted (Tables 1 and 2), whichever is the greater. All <sup>143</sup>Nd/<sup>144</sup>Nd isotope ratios were corrected to a La Jolla <sup>143</sup>Nd/<sup>144</sup>Nd ratio of 0.511850. External reproducibility of <sup>143</sup>Nd/<sup>144</sup>Nd ratios, based on replicate analyses of La Jolla Nd, is estimated to be ±0.000025 or the internal precision quoted (Tables 1 and 2), whichever is greater. Rb, Sr, Sm and Nd concentrations were determined by isotope dilution. Total procedural blanks for analyses other than of sphalerite were <3 ng Sr and <<1 ng Nd and are negligible.

The very low quantities of Rb and Sr extracted from sphalerite leachates were loaded onto single zone-refined rhenium filaments with 1 M H<sub>3</sub>PO<sub>4</sub> and a Ta<sub>2</sub>O<sub>5</sub> emitter solution. Rhenium was used instead of the more conventional tungsten, as experiments with tungsten ribbon revealed the stock tungsten in the UCD laboratory to be releasing organic material with atomic masses falling in the range of 80–90. Total procedural blanks for sphalerite Rb–Sr work were ≤1 ng Sr and ~200 pg Rb.

#### Results

Rb–Sr and Sm–Nd isotope data are given for Navan gangue minerals and sphalerite in Table 1 and for host Lower Carboniferous sedimentary rocks and sub-Carboniferous basement rocks in Table 2. Initial isotope ratios and ε<sub>Nd</sub> values have been calculated for 350 Ma, the estimated age of mineralisation, in all data tables and figures. Recalculation to different geologically reasonable ages does not significantly alter the isotopic relationships between samples nor the interpretations presented.

Carboniferous whole rocks and Navan sphalerite and gangue minerals

Within the carbonate gangue minerals, a rise in  $^{87}\text{Sr}/^{86}\text{Sr}$  ratio with time (paragenetic stage) is apparent from the unaltered host rock value of less than 0.7080 to the paragenetically latest calcite value of  $\sim 0.7100$  (Fig. 3a). The fluid inclusion leachates of four sphalerite samples are relatively unradiogenic (0.7082–0.7085) and can be viewed as a deviation away from the trend defined by the carbonates. Similarly barite, which is always relatively late in the paragenesis, falls outside this trend and possesses low  $^{87}\text{Sr}/^{86}\text{Sr}$  values marginally above those of unaltered host rock. The opposite relationship is seen for the carbonates in a plot of  $^{143}\text{Nd}/^{144}\text{Nd}$  vs paragenetic stage (Fig. 3b), in which a trend toward progressively lower  $^{143}\text{Nd}/^{144}\text{Nd}$  values over time is evident. Here, unaltered host rock has a  $^{143}\text{Nd}/^{144}\text{Nd}$  ratio of  $\sim 0.51180$ , whilst paragenetically latest calcite possesses a  $^{143}\text{Nd}/^{144}\text{Nd}$  ratio of  $\sim 0.51156$ .

There is also a correlation between initial Sr–Nd ratios and spatial position in the orebody for the gangue minerals analysed. There is a crude pattern in which more radiogenic

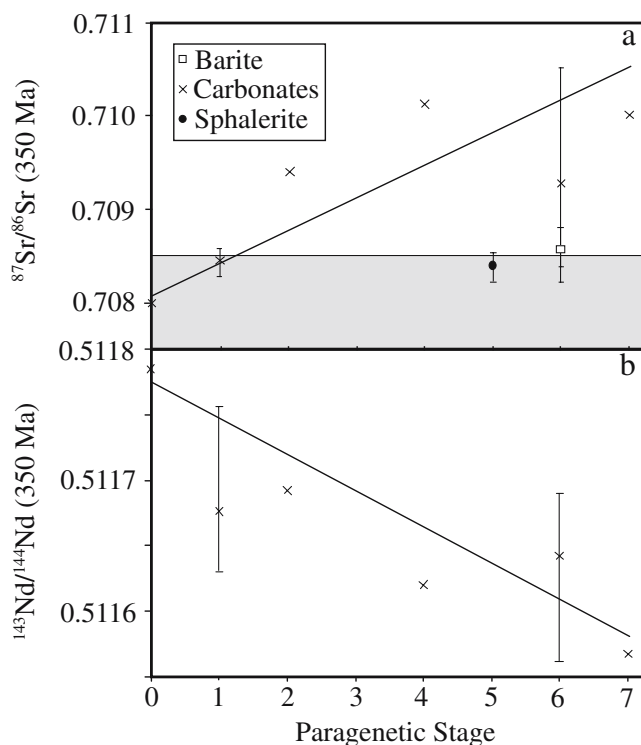


**Fig. 3** **a** Initial  $^{87}\text{Sr}/^{86}\text{Sr}$  ratios of Navan gangue minerals and sphalerite fluid inclusions (leachates) plotted against paragenetic stage (mean and range are shown where more than one sample analysed). Stippled area represents the composition of Lower Carboniferous carbonate host rocks. Carbonates display a rising trend in  $^{87}\text{Sr}/^{86}\text{Sr}$  over time. Sphalerite leachates and barites do not conform to this trend. **b** Initial  $^{143}\text{Nd}/^{144}\text{Nd}$  ratios of Navan gangue minerals plotted against paragenetic stage (mean and range are shown where more than one sample analysed)

initial  $^{87}\text{Sr}/^{86}\text{Sr}$  ratios (Fig. 4a) and less radiogenic  $^{143}\text{Nd}/^{144}\text{Nd}$  ratios (Fig. 4b) are concentrated in the higher levels of the ore deposit, typically in veins and cavity fills. The least radiogenic of the Sr isotope ratios are found in the lowermost 2–5 ore lens where massive ore is some of the richest in the body.

Two samples of unmineralised Lower Carboniferous limestone have been analysed. One (BFL7/95 from Navan) lies within the  $^{87}\text{Sr}/^{86}\text{Sr}$  range expected for seawater, the other (WTwm from Tynagh) at a slightly higher value of 0.7085. Although the  $^{143}\text{Nd}/^{144}\text{Nd}$  ratio of seawater varies at any time on Earth due to the lower residence time of Nd (Piepgras et al. 1979), the Navan and Tynagh limestones may be taken as representative. They have initial  $^{143}\text{Nd}/^{144}\text{Nd}$  ratios of 0.51178 and 0.51169, respectively.

Other whole-rock samples

Ten Old Red Sandstone samples from the Munster Basin in counties Cork and Kerry display a remarkably small range of initial  $^{143}\text{Nd}/^{144}\text{Nd}$  ratios, from 0.51172 to 0.51186. Two (ST301 and ST310) have  $^{147}\text{Sm}/^{144}\text{Nd}$  ratios  $>0.15$ , unusually high compared to typical clastic sedimentary rocks. This may be due to the presence of enough zircon to dominate their Sm–Nd budgets. There is no discernible variation related to stratigraphic or geographic position of the analysed samples. Initial  $^{87}\text{Sr}/^{86}\text{Sr}$  ratios were also determined for four samples and range from 0.7083 to 0.7170. All have  $^{87}\text{Rb}/^{86}\text{Sr}$  ratios greater than 3, consistent with their derivation largely from rocks of broadly granitic composition.

Five samples of sedimentary and metasedimentary samples from Silurian inliers in County Tipperary display initial  $^{143}\text{Nd}/^{144}\text{Nd}$  ratios of 0.51177 to 0.51186 and initial  $^{87}\text{Sr}/^{86}\text{Sr}$  ratios of 0.7097 to 0.7191. These values are similar to those determined for the Old Red Sandstone samples, though slightly higher in terms of mean  $^{87}\text{Sr}/^{86}\text{Sr}$  ratio. All have typical crustal  $^{147}\text{Sm}/^{144}\text{Nd}$  ratios in the range 0.112 to 0.118.  $^{87}\text{Rb}/^{86}\text{Sr}$  ratios range from 0.15 to 5.9, suggesting a varied provenance.

Drill core samples of presumed Ordovician volcanic and sedimentary rocks from beneath the main Navan orebody have initial  $^{143}\text{Nd}/^{144}\text{Nd}$  and  $^{87}\text{Sr}/^{86}\text{Sr}$  ratios of 0.51178 to 0.51217 and 0.7073 to 0.7186, respectively. The initial  $^{143}\text{Nd}/^{144}\text{Nd}$  ratios are notably higher than those recorded in both the Old Red Sandstone and Silurian samples analysed, though their  $^{87}\text{Sr}/^{86}\text{Sr}$  ratios are similar.

Isotopic characteristics of hydrothermal fluids

Published values for Courceyan to Arundian seawater and Courceyan Limestone  $^{87}\text{Sr}/^{86}\text{Sr}$  ratios (Bruckschen et al.

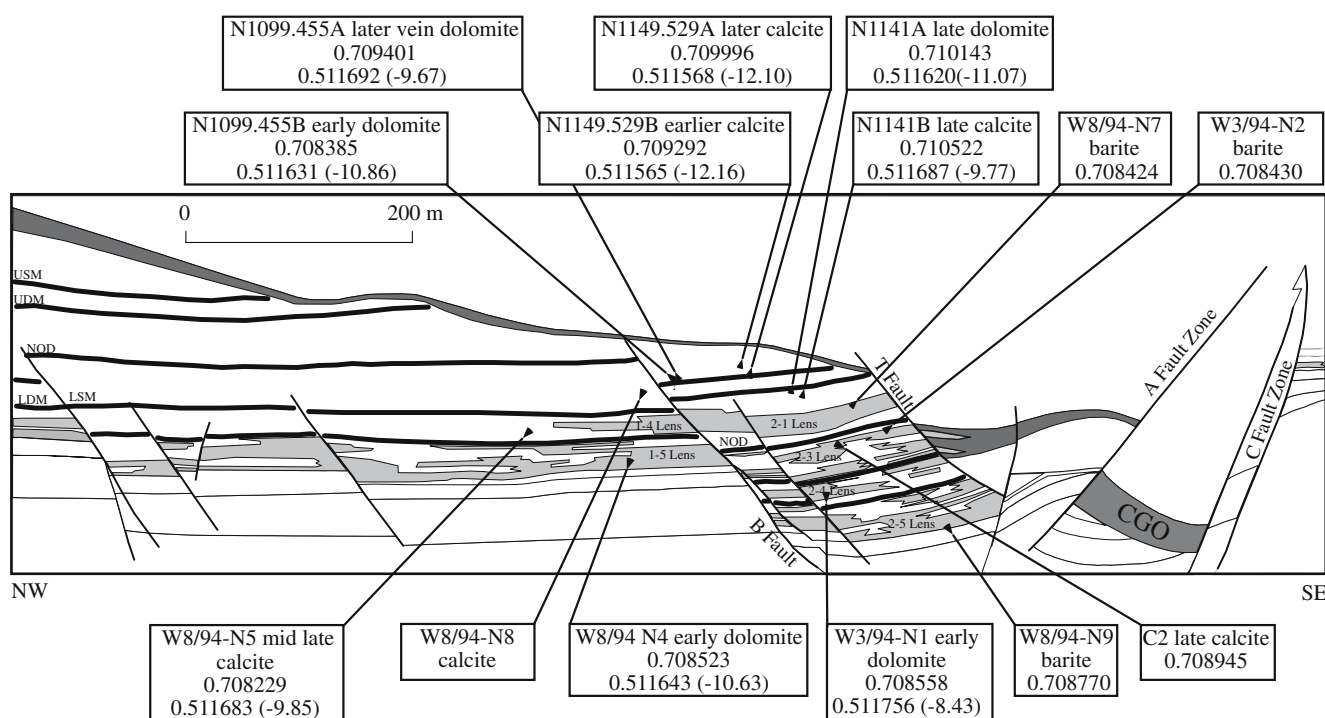


**Fig. 4** Cross section of the Navan deposit after Ashton et al. (1986), showing a schematic representation of the geometrical distribution of initial  $^{87}\text{Sr}/^{86}\text{Sr}$  (second line of labels) and initial  $^{143}\text{Nd}/^{144}\text{Nd}$  and  $\epsilon_{\text{Nd}}$

(third line of labels,  $\epsilon_{\text{Nd}}$  in parentheses) values around the ore deposit. There is a general increase in  $^{87}\text{Sr}/^{86}\text{Sr}$  and decrease in  $^{143}\text{Nd}/^{144}\text{Nd}$  ratios toward the higher levels of the orebody

1995; Douthitt et al. 1993; Popp et al. 1986) define a range from  $\sim 0.7075$  to  $\sim 0.7082$ . Accepting that the bulk of Lower Carboniferous limestones possess  $^{87}\text{Sr}/^{86}\text{Sr}$  ratios of less than 0.7082 but that the potential for higher values exists in the early Courceyan, measured  $^{87}\text{Sr}/^{86}\text{Sr}$  ratios for gangue minerals in excess of 0.7085 require introduction of Sr from another more radiogenic reservoir. Similarly, the lower initial  $^{143}\text{Nd}/^{144}\text{Nd}$  ratios of nearly all the Navan gangue minerals compared to likely seawater compositions, as shown by local limestone samples, requires another less radiogenic source of Nd. These data may thus be interpreted as showing the mixing of two fluids to create the Navan ore deposit, one with  $^{87}\text{Sr}/^{86}\text{Sr}$  and  $^{143}\text{Nd}/^{144}\text{Nd}$  ratios similar to seawater, the other with higher  $^{87}\text{Sr}/^{86}\text{Sr}$  ratio and lower  $^{143}\text{Nd}/^{144}\text{Nd}$  ratio.

There appears to be no potential source for the high  $^{87}\text{Sr}/^{86}\text{Sr}$ –low  $^{143}\text{Nd}/^{144}\text{Nd}$  ratio fluid within the post-Old Red Sandstone Lower Carboniferous succession. Most are carbonate rocks of measured or presumed seawater isotopic composition. A single sample of argillite from the Argillaceous Bioclastic Limestone (W3347) has an initial  $^{143}\text{Nd}/^{144}\text{Nd}$  ratio of 0.51152 and an initial  $^{87}\text{Sr}/^{86}\text{Sr}$  ratio of 0.7086. Although the former is low enough to be the source of less radiogenic Nd required, it cannot supply the more radiogenic Sr. Furthermore, this unit lies above the ore-bearing horizons and is not significantly hydrothermally altered, so it is highly unlikely to be a reservoir from which a hot hydrothermal fluid leached metals. During

Lower Carboniferous times the only feasible reservoirs for more radiogenic Sr and less radiogenic Nd comprise the underlying siliciclastic or metamorphic rocks, namely Lower Carboniferous clastic horizons, the Devonian Old Red Sandstone, Lower Palaeozoic and Precambrian basement rocks.

### Fluid–rock isotopic equilibrium

The isotope data are interpreted in terms of the two principal fluids identified in the Irish orefield, namely a high-temperature, metal-rich brine, here called EM1, and a cooler, more saline but metal-poor brine, here called EM2. To interpret the Sr and Nd isotope compositions of EM1, an understanding is required of the extent of isotopic equilibrium between EM1 and the rocks from which it acquired Sr and Nd. The controlling factors are fluid chemistry and the solubility of Sr- and Nd-bearing minerals in the source rocks. In addition, the possibility of differences in solubility between Sr and/or Nd and Zn and/or Pb must be considered in order to constrain base metal sources.

EM1 is considered to have been reducing, at least slightly acidic and chloride dominated (Everett et al. 1999; Russell 1986). Haas et al. (1995) and Gammons et al. (1996) concluded that under acidic conditions REE speciation is most likely to be as chloride complexes. A decrease in pH and an increase in Cl concentration, significantly increase

REE solubility in hydrothermal systems (Gammons et al. 1996). EM1, at  $>200^{\circ}\text{C}$ , represents a good solvent for Nd and the more soluble Sr.

The potential basement lithologies are mainly granitic gneisses and various sedimentary rocks, metasediments and metavolcanics. In granitic gneiss, and most other orthogneisses, the dominant hosts of Sr are likely to be the feldspars, principally plagioclase. Whilst biotite and muscovite are likely to contain radiogenic Sr with very high  $^{87}\text{Sr}/^{86}\text{Sr}$  ratios, their Sr concentrations are up to two orders of magnitude lower than plagioclase (Seimille et al. 1998). It is reasonable to assume that the  $^{87}\text{Sr}/^{86}\text{Sr}$  ratio of the whole rock will be dominated by plagioclase and K-feldspar. As these minerals are the more soluble components within granitic rocks, they will impart an  $^{87}\text{Sr}/^{86}\text{Sr}$  ratio to the hydrothermal fluid, which is similar to that of the whole rock. The likelihood of a fluid acquiring an  $^{87}\text{Sr}/^{86}\text{Sr}$  ratio substantially different to the bulk rock therefore seems low. Similar considerations apply to acid metavolcanics. In sedimentary rocks and metasediments, the major Sr hosting minerals will be feldspars, carbonates and clay minerals. These minerals are all sufficiently soluble (Bischoff et al. 1981) to render unlikely the formation of an exotic fluid  $^{87}\text{Sr}/^{86}\text{Sr}$  ratio by differential leaching. The Sr budget of basic and intermediate metavolcanics will also be overwhelmingly dominated by soluble minerals, principally plagioclase, with subordinate amounts in pyroxenes and amphiboles.

In the case of Nd, some of the REE-hosting minerals in granitic rocks, acid metavolcanics and clastic metasediments are less soluble, principally zircon and monazite (Poitrasson et al. 1995). In clastic sedimentary and metasedimentary rocks, the Nd in detrital zircon is not sufficient to produce a bias in fluid  $^{143}\text{Nd}/^{144}\text{Nd}$  ratio through its failure to dissolve, except in some very quartz-rich sedimentary and metasedimentary rocks whose Nd concentrations are, however, very low. In acid igneous rocks, the REE budget is usually dominated by the relatively soluble apatite and titanite (e.g. Condie et al. 1995). Monazite may dominate the REE budget of sedimentary and metasedimentary rocks. However, petrographic examination revealed no visible monazite in any of the Irish sedimentary or metasedimentary samples analysed. Furthermore, Read et al. (1987) report Lower Palaeozoic rocks in northern Britain to have no significant monazite REE budgets. Due to its approximately average crustal Sm/Nd ratio, monazite, even if it were present, is not likely to be out of isotopic equilibrium with its host rocks unless it had a separate provenance.

It is concluded that the Sr and Nd isotope compositions of EM1 are unlikely to be significantly different from those of the whole rocks which it has leached. Thus the composition of EM1 provides a means of constraining the

lithologies of its Sr and Nd sources. Since Zn and Pb are also likely to be overwhelmingly hosted in minerals soluble in EM1 hydrothermal fluid, principally feldspars, clay minerals and ferromagnesian silicates, these elements are very likely to have been derived from the same sources as Sr and Nd.

### Origin and mixing of fluids

A plot of  $^{87}\text{Sr}/^{86}\text{Sr}$  vs  $1/\text{Sr}$  concentration (Fig. 5a) is suggestive of mixing within a ternary system in which one end member possesses high Sr concentration and low  $^{87}\text{Sr}/^{86}\text{Sr}$  ratio, and two end members each possess lower Sr concentration but high  $^{87}\text{Sr}/^{86}\text{Sr}$  ratio. Whilst the existence of three components cannot be ruled out and is permitted by fluid inclusion data, it is thought much more likely that the apparent three-end-member relationship in Fig. 5a is an artifact of Sr having a higher mineral/fluid distribution coefficient in calcite than in dolomite. The Navan data are therefore interpreted as indicating a binary mixing system. A similar plot of  $^{143}\text{Nd}/^{144}\text{Nd}$  vs  $1/\text{Nd}$  concentration defines a cluster of points from which no significant trend is discernible (Fig. 5b).

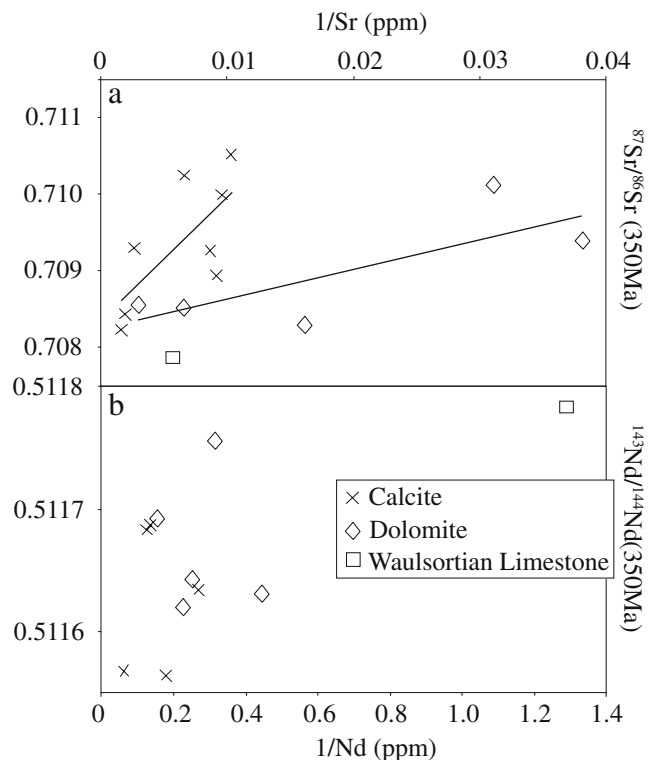


**Fig. 5** **a** Plot of initial  $^{87}\text{Sr}/^{86}\text{Sr}$  vs  $1/\text{Sr}$  concentration for Navan carbonates. Calcite and dolomite data sets each suggest binary mixing between low  $^{87}\text{Sr}/^{86}\text{Sr}$ , high Sr concentration, and high  $^{87}\text{Sr}/^{86}\text{Sr}$ , low Sr concentration end members. **b** Plot of initial  $^{143}\text{Nd}/^{144}\text{Nd}$  vs  $1/\text{Nd}$  concentration for Navan carbonates

The observed range in Sr isotope compositions of the Navan gangue minerals can be explained in terms of simple mixing between two end members. The same cannot be immediately said for the range in Nd isotope compositions. Nevertheless, it is reasonable to assume that the radiogenic Sr and unradiogenic Nd detected in late gangue samples had a common source. The paragenetic anticorrelation between Sr and Nd displayed in Fig. 3 is consistent with this. The lack of a binary mixing trend for Nd in Fig. 5b may result from substantial hosting of gangue mineral Nd budgets in fluid inclusions, whose abundance varies from sample to sample. Alternatively, it may be the case that more than two fluid components are present. However, at this point an assumption is made, namely that Nd and Sr share a common source and that the Nd isotope system possesses two end members, one of relatively high  $^{143}\text{Nd}/^{144}\text{Nd}$  and low Nd concentration and one having lower  $^{143}\text{Nd}/^{144}\text{Nd}$  and higher Nd concentration.

Assuming that Sr and Nd in each of the end members in this binary system have a common source, then the first of these end members (EM1) possesses high  $^{87}\text{Sr}/^{86}\text{Sr}$  ratio and low  $^{143}\text{Nd}/^{144}\text{Nd}$  ratio combined with relatively low Sr concentration and relatively high Nd concentration. The second of these end members (EM2) is characterised by low  $^{87}\text{Sr}/^{86}\text{Sr}$  ratio and high  $^{143}\text{Nd}/^{144}\text{Nd}$  ratio combined with a high Sr concentration and a low Nd concentration. Exactly these geochemical characteristics are possessed by Lower Carboniferous limestone and would also be possessed by any fluid that reached equilibrium with it. As no other geological unit within the Irish midlands fits the necessary criteria and because of the fact that this is the host lithology for the ore deposits, EM2 is proposed to be a fluid equilibrated with Lower Carboniferous limestone. The geochemical and isotope characteristics of EM1 might have been supplied by a number of clastic and metamorphic lithologies underlying, or potentially interbedded with, the Lower Carboniferous sequence. Identification of the source of EM1 is considered in the next section.

The anomalously low  $^{87}\text{Sr}/^{86}\text{Sr}$  ratio of sphalerite in the paragenetic sequence (Fig. 3a) may be due to the need for an influx of EM2 fluid to bring about sulphide precipitation. Since this fluid is a much more concentrated brine than EM1, it would probably contain a higher Sr concentration and, therefore, dominate the Sr budget of minerals precipitating from the fluid mixture.

Recalling the spatial variation in initial Sr and Nd isotope ratios (Fig. 4), the upper areas of the ore deposit are therefore those which experienced a higher basement to host (or EM1 to EM2) fluid ratio. As these higher EM1/EM2 ratios have been shown to occur in the later paragenetic stages, it might follow that the upper parts of the orebody formed later in the life of the hydrothermal system. If this is the case, then the lowermost sections of

the orebody in which Sr and Nd isotope ratios are unradiogenic and radiogenic, respectively, can be seen as having formed earlier in an environment in which the buffering effect of EM2 was strong. However, it must be stressed that this spatial trend in the isotope composition of gangue minerals might be more indicative of differences in fluid flow regimes rather than a difference in age of mineralisation within the orebody.

### The sources of base metals

The Nd isotope evolution of Navan gangue minerals is compared to that of Devonian Old Red Sandstones of the Munster Basin in Fig. 6. At the time of mineralisation (~350 Ma), there is little overlap between the Navan gangue and the Old Red Sandstone. Assuming again that the range of Navan gangue  $\epsilon_{\text{Nd}}$  values results from mixing of a Carboniferous limestone-equilibrated fluid of high  $\epsilon_{\text{Nd}}$  (EM2) with another fluid of lower  $\epsilon_{\text{Nd}}$  (EM1), the Old Red Sandstone can be ruled out as the source of EM1. This conclusion accords with that reached by Everett et al. (2003) through comparison of the Pb isotope compositions in the Old Red Sandstone with those of Irish ore field galenas.

The Silurian metasediments of the County Tipperary inliers have  $\epsilon_{\text{Nd}}$  values of -6.5 to -8.1 (Table 2), within the range of the Old Red Sandstone, and can also be ruled out as a source of EM1. The Cambro-Ordovician metasedimentary rocks of the Ribband Group of southeast Ireland also possess Nd too radiogenic to have been the source of EM1 (Mohr 1991). Radiogenic isotope data therefore appear to rule out derivation of a significant proportion of metals by regional fluid flow from the south.

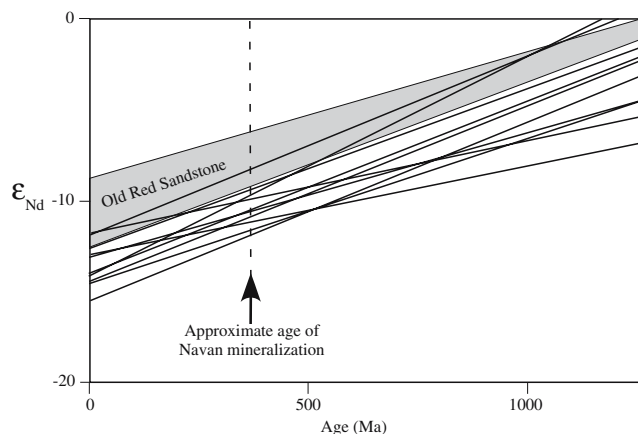


**Fig. 6**  $\epsilon_{\text{Nd}}$  vs time showing evolution of Navan gangue and Old Red Sandstone samples. Shaded area shows range of  $\epsilon_{\text{Nd}}$  evolution of samples from the Old Red Sandstone of the Munster basin. Lines indicate  $\epsilon_{\text{Nd}}$  evolution of individual samples of Navan gangue minerals

Although Sr isotopes are less reliable discriminants than Nd isotopes, further constraints on the source of EM1 can be imposed by considering Nd and Sr isotope compositions in combination. Figure 7 compares the Navan gangue Nd and Sr isotope compositions with those of a variety of sub-Carboniferous rocks. It is again apparent that the Old Red Sandstone and midlands Silurian are not feasible sources of EM1, nor are the presumed Ordovician sedimentary and volcanic rocks, which underlie the Navan deposit. A single analysis of relatively pure argillite from the Argillaceous Bioclastic Limestone overlying the Navan deposit has a low enough  $\epsilon_{Nd}$  value (−13.1) but too low a  $^{87}Sr/^{86}Sr$  ratio (0.7086) to be a source of EM1. Since the bulk of the ABL is marine carbonate rather than argillite, it is most likely that the mean  $^{87}Sr/^{86}Sr$  ratio of this unit is lower than in the analysed sample. Even if analysis of more samples demonstrated a range to much higher  $^{87}Sr/^{86}Sr$  ratios, it is hard to envisage a significant fluid contribution from the ABL as it exhibits little hydrothermal alteration in the Navan area.

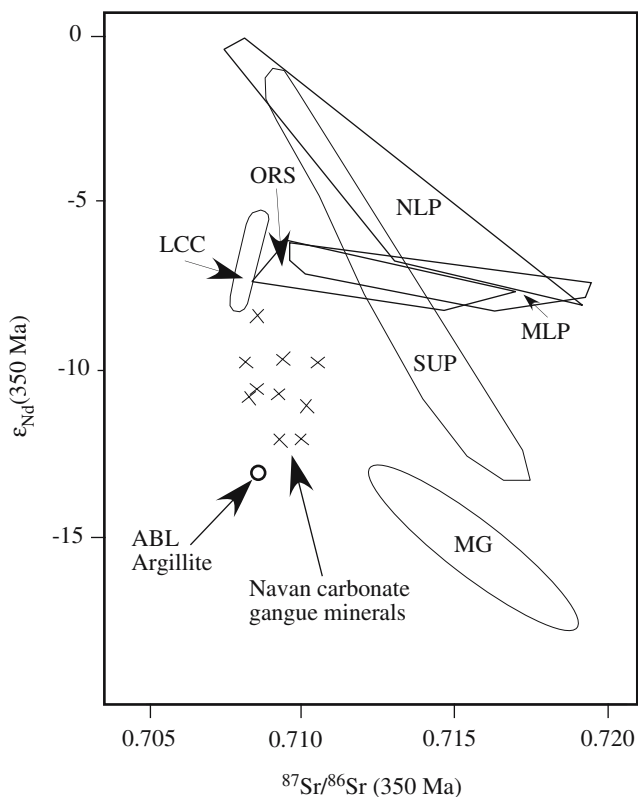


**Fig. 7** Initial  $\epsilon_{Nd}$  vs  $^{87}Sr/^{86}Sr$  for Navan carbonate gangue minerals (crosses) relative to Mullet Gneisses of the Annagh Gneiss Complex (MG), Old Red Sandstone of the Munster Basin (ORS), Lower Palaeozoic sedimentary and volcanic rocks from beneath the Navan deposit (NLP), Southern Uplands Lower Palaeozoic rocks (SUP) (Davies 1983; Stone and Evans 1995), Irish midlands Lower Palaeozoic sedimentary rocks (MLP), argillite from the Argillaceous Bioclastic Limestone and Lower Carboniferous carbonate sedimentary rocks (LCC)

However, the range of Nd and Sr isotope compositions of Lower Palaeozoic sedimentary rocks from the Southern Uplands of Scotland and of the Palaeoproterozoic Mullet Gneisses could, in principle, account for EM1. The Scottish Southern Uplands are the equivalent, along strike, of the Lower Palaeozoic rocks of the Longford-Down inlier of Ireland, whose southeast margin underlies the Navan deposit. Therefore, they may contain rocks of comparable Nd and Sr isotope composition. The Mullet Gneisses are the oldest component of the Annagh Gneiss Complex, which outcrops only in north County Mayo (Fig. 1), and are the oldest rocks known in mainland Ireland.

Binary mixing of materials with fixed isotope compositions and concentrations in the coupled Sr–Nd isotope system produces hyperbolic curves on plots of  $^{87}Sr/^{86}Sr$  ratio against  $^{143}Nd/^{144}Nd$  ratio. The curvature of such mixing lines depends on  $R$ , where  $R=(Sr/Nd)_{EM2}/(Sr/Nd)_{EM1}$ . When  $R=1$ , the mixing curve is a straight line. The greater the deviation of  $R$  from 1, the more strongly curved is the mixing trend. In the present study, the Sr and Nd concentrations and Sr/Nd ratios of the fluid end members EM1 and EM2 are unknown. Controlling factors include the Sr and Nd concentrations of the rocks leached by the fluid, Sr and Nd partition coefficients between fluid and rock, and the possibility of prior precipitation of part of the load of these elements. However, since EM2 is taken to be a limestone-equilibrated fluid, it is likely to have a higher Sr/Nd ratio than EM1, which must have passed primarily through silicate rocks of much lower Sr/Nd ratio. This conclusion is supported by a Sr/Nd ratio of ~93 obtained by a single crush-leach analysis of calcite gangue from the Lisheen Zn–Pb deposit (Walshaw, unpublished data). Consequently,  $R$  values for EM1–EM2 mixtures will exceed 1, and plausible mixing curves are restricted to those, which are convex downwards in diagrams such as Fig. 7 and where EM1 lies below and to the right of the Navan gangue data. Rocks of the Scottish Southern Uplands and the Mullet Gneisses of north Mayo are now examined as possible sources of EM1.

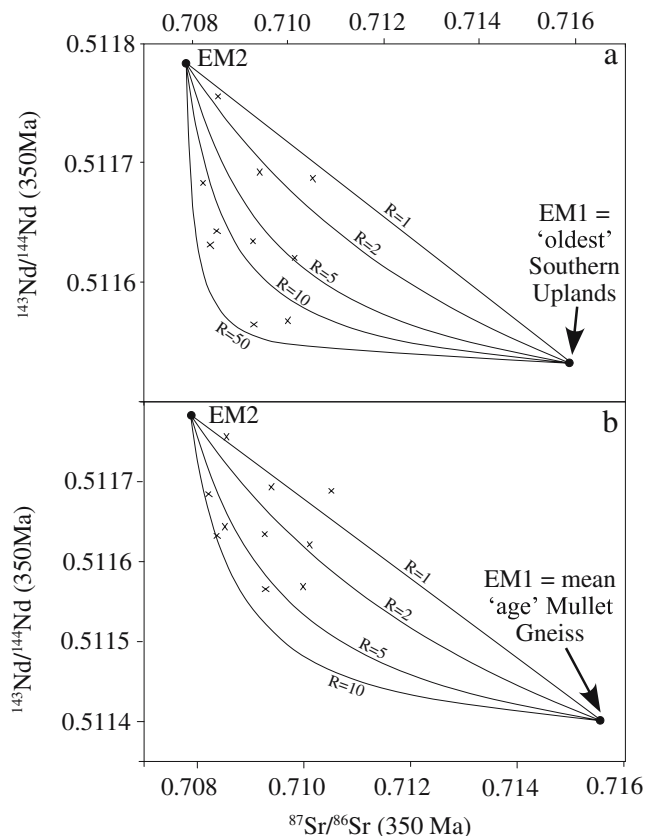
### Scottish Southern Uplands

Figure 7 demonstrates that most Lower Palaeozoic rocks of the Southern Uplands are too radiogenic in terms of Nd (Stone and Evans 1995) to represent EM1 alone. This argues against the involvement of a fluid that has pervasively scavenged the Lower Palaeozoic succession of the Longford-Down Inlier, because such involvement would be expected to introduce much more radiogenic Nd to the system than is seen. This is especially so because the Lower Palaeozoic rocks immediately beneath Navan are at the upper end of the range seen in the Southern Uplands (Fig. 7). Nevertheless, the least radiogenic Southern

Uplands sample, from the Ordovician Kirkolm Formation, could theoretically represent EM1 in terms of both Sr and Nd. Figure 8a illustrates an analysis of the relationships between Navan gangue data and binary mixing lines drawn at different  $R$  values between EM2 and Southern Uplands material with the lowest initial  $^{143}\text{Nd}/^{144}\text{Nd}$  ratio. It is evident that all Sr and Nd isotope compositions observed in the Navan gangue mineral data set could be created if the minerals precipitated from bulk hydrothermal fluids that had fluctuating  $R$  values. In this instance, the  $R$  values of the mixing lines, which create an envelope around the Navan data, range from  $\sim 30$  to  $\sim 1$ .

#### Mullet Gneiss, Annagh Gneiss Complex, north Mayo

The mean Sr and Nd isotope compositions of the Mullet Gneiss may plausibly create the observed array of Navan gangue samples through mixing with EM2. Figure 8b shows that mixing lines for  $R = \sim 0.5$  to  $\sim 10$  accommodate the Navan data. With mean Mullet Gneiss being plotted as



**Fig. 8** Isotopic mixing between fluids deriving their Nd and Sr from the sub-Carboniferous basement (fluid EM1) and from Carboniferous limestone (EM2). Mixing curves are labelled with the value of  $R$ , where  $R = (\text{Sr}/\text{Nd})_{\text{EM1}}/(\text{Sr}/\text{Nd})_{\text{EM2}}$ . Crosses show analyses of Navan gangue minerals. **a** EM1 is represented by Southern Uplands Palaeozoic shale with lowest initial  $^{143}\text{Nd}/^{144}\text{Nd}$  ratio. **b** EM1 is represented by Mullet Gneiss of mean initial  $^{143}\text{Nd}/^{144}\text{Nd}$  ratio

EM1, one Navan sample falls above the line of  $R=1$ . For the parent fluid to develop an  $R$  value of less than 1, then the Sr/Nd of EM2 must be dramatically reduced. This would best be done via the influx into the mixture of a large amount of fluid with a low Sr/Nd ratio into the system. As EM2, with an estimated Sr/Nd ratio in the order of 500–1,000, is the principal buffer in the system and EM1 most likely has a Sr/Nd ratio greater than 1, it is difficult to envisage this happening. This suggests that, although Mullet Gneiss-derived EM1 can explain the bulk of the Navan gangue data, a contribution from material of more radiogenic Nd is also required. Suitable rocks occur within the Annagh Gneiss Complex and in the Lower Palaeozoic rocks already discussed.

The Mullet Gneiss is not the only possible Proterozoic source lithology for EM1. Mullet Gneiss possesses a suitable Nd and Sr isotope character due principally to its age. Other geological units containing Nd of similar crustal residence age could equally well represent a source for EM1. These would include the Neoproterozoic Dalradian Supergroup, whose  $\epsilon_{\text{Nd}}(350 \text{ Ma})$  values range from  $-6.7$  to  $-21.3$  (Daly and Menuge 1989; Daly and Menuge, unpublished data). It is not known whether either the Annagh Gneiss Complex or the Dalradian Supergroup extend as basement beneath the Navan area.

#### Hydrothermal fluid pathways

The  $^{143}\text{Nd}/^{144}\text{Nd}$  ratio of fluid EM1 is too low to have been imparted by flow through the Devonian Old Red Sandstone of the Munster Basin of southern Ireland as required in models of regional fluid flow in response to Hercynian uplift (Hitzman 1995a,b; Figs 6 and 7). Silurian rocks of the midland inliers also have Nd that are too radiogenic to account for the composition of EM1 (Fig. 7). Irrespective of whether such regional fluid flow occurred, the hydrothermal Nd must have been derived from sub-Devonian rocks. Since older rocks are most unlikely to have been permeable enough to permit large-scale lateral fluid flow, the data require that the source of EM1 is in the sub-Devonian basement in the Navan area.

As argued in the previous section, it is doubtful in terms of mass balance that Ordovician rocks of the Longford-Down Inlier could supply sufficient Nd of this isotopic type to EM1. Two main possibilities remain regarding the source of EM1 solutes:

- EM1 fluids were derived from a mixture of the Ordovician rocks of the Longford-Down Inlier and the underlying basement, be it Mullet Gneiss, Dalradian or an unexposed unit of similar Nd isotope composition.

- (b) EM1 fluids were supplied solely by the sub-Palaeozoic basement and the isotope compositions observed in the Navan deposit were created by binary mixtures of this and EM2.

The isotope data above do not discriminate between these two processes. However, with a view to genetic models, both processes are consistent with what would be expected from a downward excavating convection cell mechanism. The gradual growth in size and volume of such a fluid flow system, as described by Russell (1986), would produce exactly the increased flux of fluid from the basement over time, which is observed in the Navan deposit (Fig. 3). Such a mechanism is also envisaged as the only one capable of accessing the deep, sub-Palaeozoic basement rocks. It equally well explains any mixing of solutes gained from these rocks with solutes gained from the overlying Ordovician rocks.

The conclusion that EM1 derived metals from Lower Palaeozoic and older rocks does not rule out the possibility that fluids that had passed through Old Red Sandstone strata ultimately made their way to the site of Navan mineralisation. It has been proposed that diagenesis of the Old Red Sandstone of the Irish midlands was due to Devonian or Lower Carboniferous meteoric water, probably driven by topographic gravity-induced flow (Hitzman et al. 2004). The possibility that such fluids later chemically and isotopically equilibrated with Lower Palaeozoic or older rocks before taking part in Navan mineralisation cannot be ruled out (LH Chapman, personal communication 2005).

## Summary

Radiogenic isotope data are interpreted primarily to indicate the mixing of two fluids: a cool, sulphide-rich, limestone-buffered brine of low  $^{87}\text{Sr}/^{86}\text{Sr}$  ratio and high  $^{143}\text{Nd}/^{144}\text{Nd}$  ratio (EM2); and a hotter, metal-bearing hydrothermal fluid of high  $^{87}\text{Sr}/^{86}\text{Sr}$  ratio and low  $^{143}\text{Nd}/^{144}\text{Nd}$  ratio, which had passed through sub-Carboniferous rocks (EM1), consistent with fluid inclusion and published S isotope data (Anderson et al. 1998). The  $^{143}\text{Nd}/^{144}\text{Nd}$  ratio of EM1 is too low to have been imparted by flow through the Devonian Old Red Sandstone of the Munster Basin of southern Ireland as required in models of regional fluid flow in response to Hercynian uplift (Hitzman 1995a,b). EM1 Nd and most of the base metals in the Navan ore deposit must have been derived from sub-Devonian rocks.

Comparison of the Navan hydrothermal gangue Nd–Sr isotope ratios with those of Lower Palaeozoic rocks strongly suggests that the latter cannot alone account for EM1. A similar conclusion was reached using Pb isotope data (O’Keefe 1986). The only known rocks occurring

NW of the Iapetus Suture in Ireland, which might supply this very unradiogenic Nd, are the Palaeoproterozoic Mullet Gneisses of the Annagh Gneiss Complex of north Mayo (Menuge and Daly 1990) and the metasedimentary rocks of the Neoproterozoic Dalradian Supergroup (Daly and Menuge 1989).

In broad terms, the convection cell model (Russell 1986) is supported, consistent with the Pb isotope compositions of Irish orefield galenas (Everett et al. 2003). Fluid flow through the largely impermeable sub-Devonian rocks beneath Navan must have been overwhelmingly along faults and fractures, but details of fluid pathways and of the source lithologies of specific metals remain to be determined. As the Navan deposit lies immediately north of the Iapetus Suture, the implication is that the Laurentian margin here includes Proterozoic basement in addition to the volcanosedimentary rocks exposed in the Longford–Down massif.

**Acknowledgements** This research was funded by Forbairt under basic research grant SC/93/004. We thank Tara Mines staff John Ashton, Billy O’Keefe, Mark Holdstock, Rob Blakeman and Jim Geraghty for providing access to mine and drill core samples and for helpful discussions at the mine.

## References

- Anderson IK, Ashton JH, Boyce AJ, Fallick AE, Russell MJ (1998) Ore Depositional Processes in the Navan Zn–Pb deposit, Ireland. *Econ Geol* 93:535–562
- Ashton JH, Downing DH, Finlay SF (1986) The geology of the Navan Zn–Pb orebody. In: Andrew CJ, Crowe RWA, Finlay S, Pennell WM, Pyne JF (eds) *Geology and genesis of mineral deposits in Ireland*. Irish Association for Economic Geology, Dublin, pp 243–280
- Ashton JH, Holdstock MP, Geraghty JF, O’Keefe WG, Martinez N, Peace W, Philcox ME (2003) In: Kelly JG, Andrew CJ, Ashton JH, Boland MB, Earls G, Fusciardi L, Stanley G (eds) *Europe’s major base metal deposits*. Irish Association for Economic Geology, Dublin, pp 405–436
- Banks DA, Russell MJ (1992) Fluid mixing during ore deposition at the Tynagh base metal deposit, Ireland. *Eur J Mineral* 4:921–931
- Banks DA, Boyce AJ, Samson IM (2002) Constraints on the origin of fluids forming Irish Zn–Pb–Ba deposits: evidence from the composition of fluid inclusions. *Geology* 97:471–480
- Bischoff JL, Radtke AS, Rosenbauer RJ (1981) Hydrothermal alteration of graywacke by brine and seawater: roles of alteration and chloride complexing on metal solubilization at 200°C and 350°C. *Econ Geol* 76:659–676
- Blakeman RJ, Ashton JH, Boyce AJ, Fallick AE, Russell MJ (2002) Timing of interplay between hydrothermal and surface fluids in the Navan Zn + Pb Orebody, Ireland: evidence from metal distribution trends, mineral textures, and  $\delta^{34}\text{S}$  analyses. *Econ Geol* 97:73–91
- Boast AM, Coleman ML, Halls C (1981) Textural and stable isotopic evidence for the genesis of the Tynagh base metal deposit, Ireland. *Econ Geol* 76:27–55
- Bonson C, Carboni V, Walsh J, Bowden A, Guven J, McDermott P, Stewart D, Whitty S (2005) Structural controls on the carbonate-hosted Lisheen and Galmoy Zn–Pb orebodies, south central

- Ireland. Abstracts, vol. 30. GAC–MAC–CSPG–CSSS Joint Meeting, Halifax, Nova Scotia, Canada, 15–18 May 2005, p 16
- Braithwaite CJR, Rizzi G (1997) The geometry and petrogenesis of hydrothermal dolomites at Navan, Ireland. *Sedimentology* 44:421–440
- Bruckschen P, Bruhn F, Veizer J, Buhl D (1995)  $^{87}\text{Sr}/^{86}\text{Sr}$  isotopic evolution of Lower Carboniferous seawater: Dinantian of western Europe. *Sediment Geol* 100:63–81
- Coller D, Beach A, Ashton J, Geraghty J, Holdstock M, O’Keeffe W, Philcox M, Walker N (2005) Structural geology and tectonic setting of the Navan Zn–Pb orebody—inversion of a degraded footwall-uplift fault block? Abstracts, vol. 30. GAC–MAC–CSPG–CSSS Joint Meeting, Halifax, Nova Scotia, Canada, 15–18 May 2005, p 31
- Condie KC, Dengate J, Cullers RL (1995) Behavior of rare earth elements in a paleoweathering profile on granodiorite in the Front Range, Colorado, USA. *Geochim Cosmochim Acta* 59:279–294
- Daly JS, Menuge JF (1989) Nd isotopic evidence for the provenance of the Dalradian Supergroup sediments in Ireland. *Terra Abstracts* 1:12
- Davies GR (1983) The isotopic evolution of the British lithosphere. Ph.D. thesis, Open University, p 276
- Douthitt TL, Meyers WJ, Hanson GN (1993) Non-monotonic variation of seawater  $^{87}\text{Sr}/^{86}\text{Sr}$  across the Ivorian/Chadian boundary (Mississippian, Osagean): evidence from marine cements within the Irish Waulsortian limestone. *J Sediment Petrol* 63:539–549
- Everett CE, Wilkinson JJ, Rye DM (1999) Fracture controlled fluid flow in the Lower Palaeozoic basement rocks of Ireland: implications for the genesis of Irish-type Zn–Pb deposits. In: McCaffrey KJW, Lonergan L, Wilkinson JJ (eds). *Fractures, fluid flow and mineralisation*. Geological Society, London, Special Publication 155:247–276
- Everett CE, Rye DM, Ellam RM (2003) Source or sink? An assessment of the role of the Old Red Sandstone in the genesis of the Irish Zn–Pb deposits. *Econ Geol* 98:31–50
- Eyre SL, Wilkinson JJ, Stanley CJ, Boyce AJ (1996) Geochemistry of dolomitisation and zinc–lead mineralisation in the Rathdowney trend, Ireland. *Geological Society of America Abstracts with Programs*, pp 210–211
- Fallick AE, Ashton JH, Boyce AJ, Ellam RM, Russell MJ (2001) Bacteria were responsible for the magnitude of the world-class hydrothermal base metal sulfide orebody at Navan, Ireland. *Econ Geol* 96:885–890
- Gammons CH, Wood SA, Williams-Jones AE (1996) The aqueous geochemistry of the rare earth elements and yttrium VI. Stability of neodymium chloride complexes from 25 to 300°C. *Geochim Cosmochim Acta* 60:4615–4630
- Garven G, Freeze RA (1984a) Theoretical analysis of the role of groundwater flow in the genesis of stratabound ore deposits: 1. Mathematical and numerical model. *Am J Sci* 284:1085–1124
- Garven G, Freeze RA (1984b) Theoretical analysis of the role of groundwater flow in the genesis of stratabound ore deposits: 2 quantitative results. *Am J Sci* 284:1125–1174
- Gleeson SA, Banks DA, Everett CE, Wilkinson JJ, Samson IM, Boyce AJ (1999) Origin of mineralising fluids in Irish-type deposits: Constraints from halogens. In: Stanley CJ et al (eds) *Mineral deposits: processes to processing*. Balkema, Rotterdam, pp 857–860
- Haas JR, Shock EL, Sassani DC (1995) Rare earth elements in hydrothermal systems: Estimates of standard partial molal thermodynamic properties of aqueous complexes of the rare earth elements at high pressures and temperatures. *Geochim Cosmochim Acta* 59:4329–4350
- Hitzman MW (1995a) Geological setting of the Irish Zn–Pb–(Ba–Ag) orefield. In: Anderson K, Ashton J, Earls G, Hitzman M, Tear S (eds) *Irish carbonate-hosted Pb–Zn deposits*. Society of Economic Geologists, Guidebook Series vol. 21. pp 3–23
- Hitzman MW (1995b) Mineralization in the Irish Zn–Pb–(Ba–Ag) orefield. In: Anderson K, Ashton J, Earls G, Hitzman M, Tear S (eds) *Irish carbonate-hosted Pb–Zn deposits*. Society of Economic Geologists, Guidebook Series, vol. 21. pp 25–61
- Hitzman MW, Large D (1986) A review and classification of the Irish carbonate-hosted base metal deposits. In: Andrew CJ, Crowe RWA, Finlay S, Pennell WM, Pyne JF (eds) *Geology and genesis of mineral deposits in Ireland*. Irish Association for Economic Geology, Dublin, pp 217–238
- Hitzman MW, Chapman LH, Humphrey J, Harrison W (2004) Lithostratigraphy, diagenesis and carbonate cement isotope characterization of Upper Devonian Old Red Sandstone; implications for fluid flow during diagenesis. *Geological Society of America Abstracts with Programs* 36:460–461
- Lydon JW (1986) Models for the generation of metalliferous hydrothermal systems within sedimentary rocks and their applicability to the Irish Carboniferous Zn–Pb deposits. In: Andrew CJ, Crowe RWA, Finlay S, Pennell WM, Pyne JF (eds) *Geology and genesis of mineral deposits in Ireland*. Irish Association for Economic Geology, Dublin, pp 555–577
- Menuge JF (1988) The petrogenesis of massif anorthosites: a Nd and Sr isotopic investigation of the Proterozoic of Rogaland/Vest-Agder, SW Norway. *Contrib Mineral Petrol* 98:363–373
- Menuge JF, Daly JS (1990) Proterozoic evolution of the Erris Complex, northwest Mayo, Ireland: neodymium isotope evidence. In: Gower CF, Rivers T, Ryan B (eds) *Mid-Proterozoic Laurentia-Baltica*. Geological Association of Canada Special Paper 38:41–52
- Mohr P (1991) Origin and cooling history of the Leinster Granite: an isotopic study. Ph.D. thesis, National University of Ireland, p 189
- Nagy ZR, Somerville ID, Gregg JM, Becker SP, Shelton KL (2005) Lower Carboniferous peritidal carbonates and associated evaporites adjacent to the Leinster Massif, southeast Irish Midlands. *Geol J* 40:173–192
- O’Keeffe WG (1986) Age and postulated source rocks for mineralisation in central Ireland, as indicated by lead isotopes. In: Andrew CJ, Crowe RWA, Finlay S, Pennell WM, Pyne JF (eds) *Geology and genesis of mineral deposits in Ireland*. Irish Association for Economic Geology, Dublin, pp 617–624
- O’Keeffe WG (1987) A regional lead isotope investigation of mineralization in Ireland. Ph.D. thesis, National University of Ireland, p 261
- Peace WM, Wallace MW (2000) Timing of mineralization at the Navan Zn–Pb deposit: A post Arundian age for Irish mineralization. *Geology* 28:711–714
- Philcox ME (1984) Lower Carboniferous Lithostratigraphy of the Irish Midlands. Special Publication, Irish Association for Economic Geology, Dublin, p 89
- Phillips WJ (1983) Discussion of Boyce et al. (1983). *Trans Inst Min Metall* 92:B102
- Phillips WEA (2001) Caledonian Deformation. In: Holland CH (ed) *The geology of Ireland*. Academic, pp 179–199
- Piepgras DJ, Wasserburg GJ, Dasch EJ (1979) The isotopic composition of Nd in different ocean masses. *Earth Planet Sci Lett* 45:223–236
- Pin C, Briot D, Bassin C, Poitrasson F (1994) Concomitant separation of strontium and samarium–neodymium for isotopic analysis in silicate samples, based on specific extraction chromatography. *Anal Chim Acta* 298:209–217
- Poitrasson F, Pin C, Duthou DL (1995) Hydrothermal remobilization of rare earth elements and its effect on Nd isotopes in rhyolite and granite. *Earth Planet Sci Lett* 130:1–11
- Popp BN, Podosek FA, Brannon JC, Anderson TF, Piper J (1986)  $^{87}\text{Sr}/^{86}\text{Sr}$  ratio in Permo–Carboniferous seawater from the

- analyses of well-preserved brachiopod shells. *Geochim Cosmochim Acta* 50:1321–1328
- Read D, Cooper DC, McArthur JM (1987) The composition and distribution of nodular monazite in the Lower Palaeozoic rocks of Great Britain. *Mineral Mag* 51:271–280
- Russell MJ (1973) Base-metal mineralization in Ireland and Scotland and the formation of Rockall Trough. In: Tarling, DH, Runcorn SK (eds) *Implications of continental drift to the earth sciences*, vol. 1. Academic, London, pp 581–597
- Russell MJ (1978) Downward-excavating hydrothermal cells and Irish-type ore deposits: importance of an underlying thick Caledonian prism. *Trans Inst Min Metall* 87:B168–B171
- Russell MJ (1986) Extension and convection: a genetic model for the Irish Carboniferous base metal and barite deposits. In: Andrew CJ, Crowe RWA, Finlay S, Pennell WM, Pyne JF (eds) *Geology and genesis of mineral deposits in Ireland*. Irish Association for Economic Geology, Dublin, pp 545–554
- Samson IM, Russell MJ (1987) Genesis of the Silvermines zinc–lead–barite deposit, Ireland: Fluid inclusion and stable isotope evidence. *Econ Geol* 82:371–394
- Seimille F, Zuddas P, Michard G (1998) Granite-hydrothermal interaction: a simultaneous estimation of the mineral dissolution rate based on the isotopic doping technique. *Earth Planet Sci Lett* 157:183–191
- Stone P, Evans JA (1995) Nd-isotope study of provenance patterns across the British sector of the Iapetus Suture. *Geol Mag* 132:571–580
- Strogen P, Somerville ID, Pickard NAH, Jones GLI, Fleming M (1996) Controls on ramp, platform and basinal sedimentation in the Dinantian of the Dublin Basin and Shannon Trough, Ireland. In: Strogen P, Somerville ID, Jones GLI (eds) *Recent advances in Lower Carboniferous Geology*. Geological Society Special Publication 107:263–279
- Symons DTA, Smethurst MT, Ashton JH (2002) Paleomagnetism of the Navan Zn–Pb Deposit, Ireland. *Econ Geol* 97:997–1012
- Vaughan A (1991) The Lower Palaeozoic geology of the Iapetus Suture zone in eastern Ireland. Ph.D. thesis, Trinity College Dublin, p 237
- Walshaw RD, Menuge JF (1998) Dating of crustal fluid flow by the Rb–Sr isotopic analysis of sphalerite: a review. In: Parnell J (ed) *Dating and duration of fluid flow and fluid–rock interaction*. Geological Society Special Publication 144:137–143
- Wilkinson JJ (2003) On diagenesis, dolomitisation and mineralisation in the Irish Zn–Pb orefield. *Miner Depos* 38:968–983
- Williams B, Brown C (1986) A model for the genesis of Zn–Pb deposits in Ireland. In: Andrew CJ, Crowe RWA, Finlay S, Pennell WM, Pyne JF (eds) *Geology and genesis of mineral deposits in Ireland*. Irish Association for Economic Geology, Dublin, pp 579–590